

## Second Harmonic Generation of Femtosecond Laser Pulses under Raman–Nath Nonlinear Diffraction

A. M. Vyunishev<sup>a, b</sup>, Yu. A. Sheremet'eva<sup>b</sup>, B. A. Nasedkin<sup>b</sup>, I. S. Baturin<sup>c, d</sup>,  
A. R. Akhmatkhanov<sup>c, d</sup>, and V. Ya. Shur<sup>c, d</sup>

<sup>a</sup>Kirensky Institute of Physics, Siberian Branch, Russian Academy of Sciences, Krasnoyarsk, 660036 Russia

<sup>b</sup>Siberian Federal University, Krasnoyarsk, 660041 Russia

<sup>c</sup>Ural Federal University, Ekaterinburg, 620002 Russia

<sup>d</sup>OOO Labfer, Ekaterinburg, 620014 Russia

e-mail: vyunishev@iph.krasn.ru

**Abstract**—The second harmonic generation of femtosecond laser pulses under Raman–Nath nonlinear diffraction in periodic domain structures of lithium niobate is considered. A theoretical model of Cherenkov nonlinear diffraction is used to calculate the spectral–angular characteristics of the second harmonic generation of femtosecond laser pulses under Raman–Nath nonlinear diffraction. Reliability of the results is confirmed by the experimental data.

DOI: 10.3103/S106287381502032X

### INTRODUCTION

Periodic quadratically nonlinear optical media are promising for the nonlinear-optical conversion of laser radiation. The periodicity of the structure determines a discrete set of vectors of the reciprocal lattice enabling us to attain quasi-phase-matching in cases where nonlinear optical conversion is impossible under the conditions of angular phase-matching. Such types of phase-matching as quasi-phase-matching, Cherenkov nonlinear diffraction [1–5], and Raman–Nath nonlinear diffraction [2–4, 6, 7] are realized in periodic structures. The last two types of phase-matching are classified as noncollinear interaction and are described by the general theoretical model in [1]. These processes are distinct in that the Cherenkov nonlinear diffraction is observed when the longitudinal components of the interacting wave vectors are matched while the Raman–Nath nonlinear diffraction occurs when the tangential components are matched. Simultaneous fulfillment of these conditions results in full vector phase-matching known as the Bragg nonlinear diffraction. Raman–Nath nonlinear diffraction is the least known of the above processes; it was observed experimentally in the form of a number of second harmonic (SH) beams generated at low angles to the incident radiation at the fundamental frequency. The practical value of this phenomenon is that it allows us to develop devices for the multiplexing (spatial separation) of laser beams. The problem of the absence of full phase-matching, which is responsible for the oscillatory character of the dependence of the second harmonic signal along a nonlinear medium and thus low conversion efficiency, has therefore to be solved. The situation is complicated by the susceptibil-

ity of the most widely used nonlinear media to photorefractive effects at moderate power densities of the incident radiation in the case of nanosecond pulses. In contrast, the use of femtosecond pulses is characterized by higher threshold values of the development of photorefractive effects. The aim of this work was therefore to conduct experimental and theoretical investigations of the second harmonic generation (SHG) of femtosecond laser pulses under Raman–Nath nonlinear diffraction.

### THEORY OF NONLINEAR DIFFRACTION

The Raman–Nath nonlinear diffraction is a phenomenon often observed in Cherenkov nonlinear diffraction. The difference between these phenomena can be easily explained if we consider the diagram of phase-matching in a periodic structure (Fig. 1). For convenience, let us separately consider matching of the longitudinal (along the wave vector of the fundamental radiation) and transverse (orthogonal to the wave vector of the fundamental radiation) components of the wave vectors of interacting waves  $k_j$  at the fundamental ( $j = 1$ ) and doubled ( $j = 2$ ) frequency. Note that with propagation of the fundamental radiation normal to the plane of vectors of the reciprocal lattice  $G_x$ , the latter are only found in the condition on transverse components that ensures a discrete set of spatial harmonics  $G_x = mG_0$ . We may therefore expect second harmonic generation in the directions corresponding to the set of spatial harmonics. However, this process would be inefficient because of the phase mismatch of the longitudinal components. The signal of the second harmonic would thus oscillate along the

nonlinear medium in a manner similar to that of the second harmonic signal in a homogeneous nonlinear medium in the absence of angular phase-matching. As the angle of propagation increases, the phase mismatch of the longitudinal components  $\Delta k_{\parallel}$  is reduced, reaching zero in the direction of equality for the projection of the wave vector for the second harmonic onto the doubled wave vector of the fundamental radiation. This is the direction of the Cherenkov nonlinear diffraction. Unfortunately, this process is also inefficient, since this direction as a rule lies in the region of high spatial harmonics (order of quasi-phase-matching  $m$ ), which are characterized by low Fourier amplitudes. In addition, there is generally no full matching of transverse components ( $\Delta k_{\perp} \neq 0$ ). Otherwise, Bragg nonlinear diffraction would occur ( $\Delta k_{\perp, \parallel} = 0$ ). Angular adjustment of the periodic structure relative to the direction of propagation of the fundamental beam [4] or tuning the fundamental radiation by frequency enables us to employ this process. The interrelation of the phenomena under consideration leads us to believe that they are described in terms of the same theoretical model for nonlinear diffraction in regular domain structures [1]. This model enabled the researchers to describe the Cherenkov nonlinear diffraction and find agreement between calculated spectral and angular dependences of the generated radiation and the ones actually measured [1, 5]. In this work, the above theoretical model is used to describe the Raman–Nath nonlinear diffraction of femtosecond pulses in a periodic domain structure in a lithium niobate crystal.

Let the fundamental radiation propagates in the positive direction of axis  $y$  that lies in the plane of domain boundaries and the sign of the nonlinear coupling coefficient of interacting waves be described by a periodic function of the transverse coordinate  $g(x)$  with period  $\Lambda$ , as is shown in Fig. 1a. We consider the case of a periodic structure with unequal thicknesses of neighboring domains. We introduce the duty cycle  $D = l_+/(l_+ + l_-)$ , where  $l_{\pm}$  denote the thicknesses of the positive and negative domains forming the period  $\Lambda = l_+ + l_-$  as a characteristic of the structure. In the approximation of slowly varying amplitudes and low conversion efficiency, the spectral density of SH intensity has the form [1]

$$S(\Omega, K, y) = (|\alpha y|)^2 \exp\left(-\frac{\tau^2 \Omega^2}{4}\right) \times \text{sinc}\left(\frac{y}{2}\left[\Delta k + v\Omega - \frac{K^2}{2k_2}\right]\right)^2 R(K), \quad (1)$$

where  $\alpha = (\pi/2)^{3/2} \tau a^2 \Gamma$ ,  $\Gamma = -i\beta_2 I_1$ ,  $\beta_2 = 2\pi k_2 \chi^{(2)}/n_2^2$ , and  $I_1$  is the maximum intensity of the fundamental radiation;  $2\tau$  and  $a$  are the pulse duration and radius of the focal spot of the fundamental radiation at the field amplitude level  $e^{-1}$ ;  $\Delta k = 2k_1 - k_2$  is the mismatch of the wave vectors at fundamental  $\omega_1$  and doubled  $\omega_2$  frequency;  $\Omega = \omega_2 - 2\omega_{10}$  is the frequency detuning

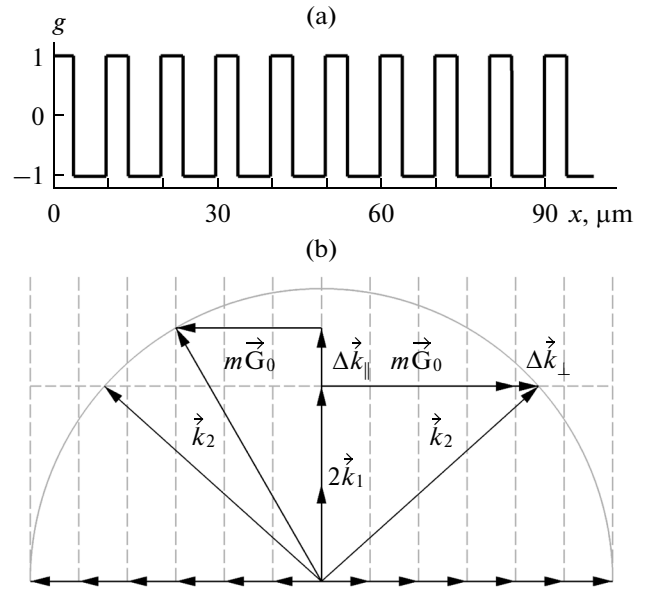


**Fig. 1.** (a) Function  $g(x)$  characterizing the variation in the sign of the nonlinear coefficient of wave coupling in the periodic structure; axis  $y$  is directed perpendicular to the figure plane. (b) Diagram of phase mismatch.

from the central frequency of fundamental radiation  $\omega_{10}$ ;  $v = (u_2^{-1} - u_1^{-1})$  is the group velocity mismatch;  $\chi^{(2)}$  is the second-order effective nonlinear susceptibility; and  $n_j$  denotes the refractive index of the material at frequency  $j\omega_1$  ( $j = 1, 2$ ) [8]. Product  $v\Omega$  corresponds to the first approximation of the dispersion theory, being responsible for the delay of pulses due to detuning of inverse group velocities. The function

$$R(K) = \left( \sum_m g_m \exp\left[-a^2 (mG_0 + K)^2/8\right] \right)^2 \quad (2)$$

is the Fourier transform of the periodic structure within the limits of propagation of the fundamental beam, where  $K$  and  $G_0 = 2\pi/\Lambda$  are the spatial frequency and modulus of the basic vector of the reciprocal lattice. Fourier coefficients  $g_m$  for the periodic lattice with the duty cycle  $D$  have the form

$$g_m = \begin{cases} 2D - 1, & m = 0 \\ 2 \sin(\pi m D)/\pi m, & m \neq 0, \end{cases} \quad (3)$$

where  $m = 0, \pm 1, \pm 2, \dots$  is the order of quasi-phase-matching. In practice, it is convenient to use the full beam size measured at half-width  $w = (2\ln 2)^{1/2} a$ . To calculate the spectral–angular SHG dependences, it is convenient to move from spatial frequencies to angles  $\theta$  of propagation of the spectral components inside a structure using the ratio  $K = 4\pi n_2 \sin(\theta)/\lambda$ , where  $\lambda$  is the wavelength of fundamental radiation.

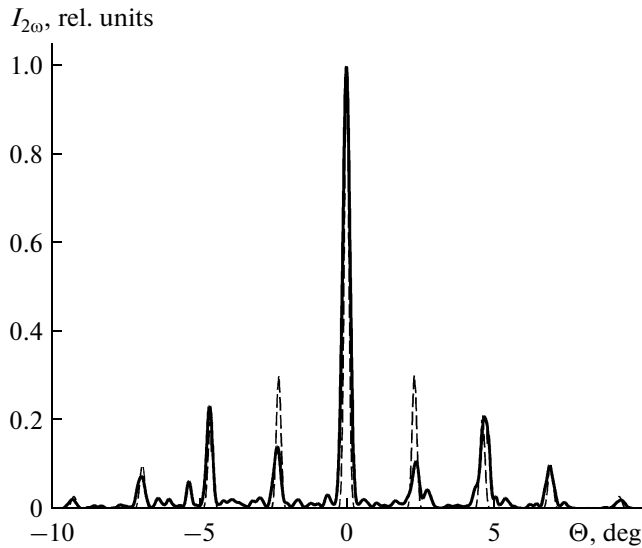


**Fig. 2.** Measured (solid line) and calculated (dashed line) angular dependences of the average power of the second harmonic pumped by fundamental radiation with a central wavelength of 800 nm.

## RESULTS AND DISCUSSION

A lithium niobate crystal of congruent composition containing a periodic domain structure served as object of our study. The sample was  $11 \times 2 \times 0.5 \text{ mm}^3$  in size. The sign of the nonlinear susceptibility was modulated along the crystallographic axis  $x$  with a period of  $10 \text{ }\mu\text{m}$  and a duty cycle ratio of  $\sim 0.8$ . Ti:sapphire femtosecond laser radiation with the average power  $\sim 600 \text{ mW}$  (pulse duration  $\tau_{1/2} = 80 \text{ fs}$ ; repetition rate  $f = 80 \text{ MHz}$ ) was focused along the crystallographic axis  $y$  using a lens with a focal length of  $20 \text{ cm}$ . The size of the focal spot was  $w = 80 \text{ }\mu\text{m}$ . Polarization of the fundamental radiation coincided with the crystallographic axis  $z$  so that we could use maximum nonlinear coefficient  $d_{33}$  of lithium niobate. The generated second harmonic spectra were detected using a Solar MSDD1000 spectrometer with an inverse linear dispersion of  $0.826 \text{ nm/mm}$  in the spectral range of interest.

Figure 2 shows the measured angular dependence of the average second harmonic power and the corresponding calculated curve found using expression (1), averaged over the spectrum and plotted on the scale of the angle of propagation  $\Theta$  outside the sample. The experimental curve was found via the translation of a narrow slit transversely relative to the direction of propagation of the fundamental radiation with simultaneous measurement of the average transmitted SH power using a Newport 918D power meter. The radiation of the second harmonic was filtered out using a BG39 filter that absorbed the fundamental radiation. Individual peaks correspond to different orders of quasi-phase-matching  $m$ . The calculated dependence was found using the parameters corresponding to the

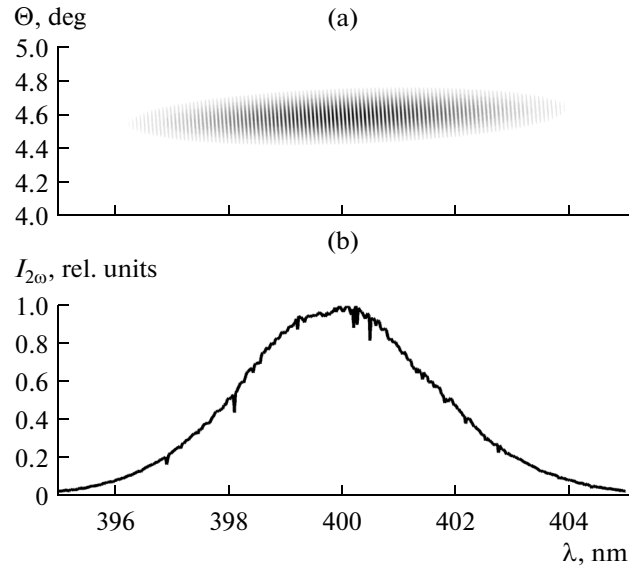


**Fig. 3.** (a) Calculated angular dependence of the spectral density of the second harmonic ( $m = 2$ ); (b) measured spectrum of the second harmonic ( $m = 2$ ).

experimental conditions. The optimal magnitude of the duty cycle value was 0.82, which agrees with the value of 0.8 measured using an optical microscope. Good agreement between the angular position of the beams and their angular widths and amplitudes was observed. A slight divergence of the amplitudes was observed for the first-order beams; this can be attributed to imperfection of the periodic structure (i.e., by local disturbance of the structure periodicity). We experimentally observed second harmonic beams corresponding to the first five orders. The maximum average power of the central beam was  $1 \text{ }\mu\text{W}$ , which corresponds to  $10^{-6}$  when recalculated into conversion efficiency.

Figure 3a shows the calculated angular dependence of the spectral density of the second harmonic for order  $m = 2$ . This dependence has the form of a spike, which is explained by the oscillatory behavior of the second harmonic signal in the nonlinear medium. The maxima correspond to spectral components for which the length of nonlinear optical interaction equals an odd number of coherent lengths. Otherwise, spectral intensity minima are observed. The group velocity mismatch  $v$  in expression (1) contributes to this dependence. This results in narrower spectral spikes and shorter distance between them. Under problem conditions, the width of spectral spikes was approximately  $0.01 \text{ nm}$  and the distance between them was  $0.06 \text{ nm}$ . Unfortunately, we failed to resolve the spike structure of the second harmonic spectra experimentally because of the weak signal and associated necessity to increase the width of the input slit of the spectrometer. Figure 3b shows the measured second harmonic spectrum. It is evident that angle averaging of

the calculated dependence in Fig. 3a within the spectral range (equal to the spectral resolution of the spectrometer under the experimental conditions) will smoothen the second harmonic spectrum.

As a rule, the use of optical elements (including lenses) increases the duration of femtosecond pulses. However, this effect does not play a large role under the problem conditions since the expression (1) for the SH field amplitude contains a spectral envelope that corresponds to the duration of the initial pulses, assuming that they are spectrally limited. Introducing new elements into the optical scheme spreads the wave packets over time (the pulse duration increases). From this instant on, the pulses are not limited spectrally but the shapes of their spectra and spectral widths remain the same. In an experiment, this should lower the efficiency of conversion and leave the spectral characteristics of the generated radiation unaffected.

Another feature of the dependence in Fig. 3a is that the spectral components are shifted into the long-wavelength region as the angle of propagation increases; i.e., the longwave components propagate at a higher angle than the shortwave components. Such dependences are normally classified according to their angular chirp. In our case, the nature of the angular chirp can be explained using the Raman–Nath condition written in a scalar form:  $\sin\theta_m = m\lambda/\Lambda$ , which can be easily derived by analyzing Eqs. (1) and (2). It is important that the angular chirp grows along with the order of quasi-phase-matching.

### CONCLUSIONS

The second harmonic generation of femtosecond laser pulses under the Raman–Nath diffraction has been investigated in periodic domain structures of lithium niobate. Angular dependences of the spectral density of the second harmonic have been calculated

using analytical expressions for Cherenkov nonlinear diffraction considering lower orders of quasi-phase-matching. The calculated integral characteristics agree with the measured quantities.

### ACKNOWLEDGMENTS

This work was supported by the Grant of the President of the Russian Federation MK-250.2013.2; by RFBR Grant No 15-02-03838; Krasnoyarsk Regional Fund for Science and Technical Activity Support; and by the Russian Academy of Sciences, Project no. 24.31.

A.R. Akhmatkhanov is grateful for the support given to young scientists under the Developmental Program of the Ural Federal University.

### REFERENCES

1. Shutov, I.V., Ozheredov, I.A., Shumitski, A.V., and Chirkin, A.S., *Opt. Spektrosk.*, 2008, no. 105, p. 87.
2. Saltiel, S.M., Neshev, D.N., Fischer, R., et al., *Phys. Rev. Lett.*, 2008, vol. 100, p. 103902.
3. Saltiel, S.M., Neshev, D.N., Krolikowski, W., et al., *Opt. Lett.*, 2009, vol. 34, p. 848.
4. Kalinowski, K., Roedig, P., Sheng, Y., et al., *Opt. Lett.*, 2012, vol. 37, p. 1832.
5. Vyunishev, A.M., Aleksandrovsy, A.S., Zaitsev, A.I., and Slabko, V.V., *Appl. Phys. Lett.*, 2012, vol. 101, p. 211114.
6. Chen, Y., Dang, W., Zheng, Y., et al., *Opt. Lett.*, 2013, vol. 38, p. 2298.
7. Sheng, Y., Kong, Q., Wang, W., et al., *J. Phys. B*, 2012, vol. 45, p. 055401.
8. Jundt, D.H., *Opt. Lett.*, 1997, vol. 22, p. 1553.

*Translated by N. Korovin*